Section 2.0 : Construction and Measurement of a Simple Test Transmission Line

After deciding to use a Focal 8V 4412 mid-bass driver for my first transmission line design, I started looking for a simple enclosure in which to perform some testing to correlate my mathematical model. I came across a 48" long cardboard tube with a 7¼" inner diameter and ¼" wall thickness at my local hardware store. For five dollars I had a test transmission line enclosure. At one end of the tube I attached a nine inch square piece of ¾" thick plywood with a circular cutout that fit snuggly over the tube's outer diameter. To secure this plywood flange, nails were driven outward through the tube into the plywood at eight locations. The seam was sealed on both sides with silicon caulk. The Focal 8V 4412 driver was mounted to the flange with a length of speaker cable threaded out through the open end of the tube. Figure 2.1 shows the test transmission line set-up.

The first test I ran, after breaking in the drivers, was to determine the Thiele / Small parameters of the Focal 8V 4412 using Liberty Instrument's Audiosuite measurement program LAUD. Table 2.1 shows the results of these measurements along with the manufacturer's specifications.

Table 2.1 : Measured Thiele / Small Parameters of the Focal 8V 4412

Property	Spec.	Average	Driver 1	Driver 2	Units
f_d	27.4	33.7	33.0	34.3	Hz
V_{ad}	105.9	66.9	67.8	65.9	liters
Q_{td}	0.30	0.38	0.38	0.37	
Q_{ed}	0.33	0.44	0.44	0.44	
Q_{md}	2.90	2.57	2.66	2.47	
R_e	7.7	7.7	7.7	7.7	ohm
S_d	221.7				cm^2
C_{ad} (10^{-7})	7.54	4.83	4.89	4.76	m^5/N
M_{ad}	44.8	46.5	47.7	45.2	kg/m^4
R_{ad}	2657	3829	3717	3941	N sec/m^5
C_{md} (10^{-3})	1.53	0.98	0.99	0.97	m/N
M_{md}	22.0	22.8	23.4	22.2	gm
R_{md}	1.306	1.882	1.827	1.937	gm/sec
C_{med}	248.4	270.2	274.7	265.6	μF
L_{ced}	135.9	82.9	84.8	81.0	mH
R_{ed}	67.8	45.0	46.7	43.2	ohm
Bl	9.4	9.2	9.2	9.1	N/amp

After determining the Thiele / Small parameters for the Focal 8V 4412 drivers, Driver 2 was mounted in the test transmission line enclosure. At this point the tube was completely empty. Three separate measurements were made. The first measurement was of the impedance of the driver mounted in the tube. The second and third measurements were of the SPL directly in front of the driver and the SPL at the terminus of the tube. For the SPL measurements, the microphone was mounted as close to the driver and terminus as possible to eliminate any reflections that might be generated from the floor or the baffle. The microphone was placed ¼" in front of the center of the driver dust cap and then out ¼" axially, along the centerline, from the terminus end of the tube.

The results of these measurements are shown in Figure 2.2. The top plot is the magnitude and phase of the system impedance. The middle plot is the SPL and phase of the woofer response. The bottom plot is the SPL and phase of the terminus response. Each plot contains a title describing the measurement being presented. Each plot also contains the sampling rate and sample size used during the measurement. For all of the frequency response plots, ten measurements were averaged to get the final data.

The measurements were repeated after stuffing the tube with 100 gm, 200 gm, and 300 gm of Dacron Hollofil II fiber. To stuff the tube, I made a 48" long cheese-cloth cylinder and tied the ends closed with string. To add or remove stuffing, the cheese-cloth cylinder was pulled out of the cardboard tube, untied, and unrolled flat. This technique made it easy to adjust the amount and type of stuffing in the test transmission line. Figures 2.3, 2.4, and 2.5 show the results of the measurements for 100 gm, 200 gm, and 300 gm of Dacron Hollofil II stuffing. The format of the plots is the same as described for Figure 2.2.

I studied the measurement results to try and understand the behavior of the test transmission line. I started with the unstuffed measurements shown in Figure 2.2. A lot can be learned from these three plots. First, I calculated the quarter wavelength modes of the tube after including an end correction to the tube length corresponding to an unflanged exit boundary condition. The ¼ wavelength calculation is shown below.

L_{tube} = 48.25" = 1.226 m
$L_{effective}$ = 48.25" + 0.6 x 3.625" = 1.281 m

$f = c / (4\ L_{effective})$ = 67 Hz
c_{air} = 342 m/sec

Table 2.2 shows the driver resonant frequency, the calculated tube quarter wavelength frequencies, and the measured system peaks from the plots in Figure 2.2.

Table 2.2 : Calculated and Measured Frequencies for the Unstuffed Test Line

Mode	Measured Driver Resonance (Hz)	Calculated Tube Frequencies (Hz)	Measured System Frequencies (Hz)
Driver	34		22
1/4 Wavelength		67	94
3/4 Wavelength		200	214
5/4 Wavelength		334	343
7/4 Wavelength		467	475
9/4 Wavelength		601	598
11/4 Wavelength		734	727

The first thing I noticed in Figure 2.2 was a shift of the driver resonant frequency in the impedance curve. The driver resonant frequency of approximately 34 Hz, as reported in Table 2.1, dropped to 22 Hz when the driver was mounted in the test transmission line. I attribute this change in frequency to an additional mass loading on the speaker cone from the air moving in the transmission line. At this low frequency, the air in the transmission line acts like a solid slug of mass. Using the value of M_{md} from Table 2.1 and the mass of air in the tube, the lowest system resonant frequency can be estimated and compared to the measured value.

$$M_{md} = 22.2 \text{ gm}$$

$$\begin{aligned} M_{air} &= \rho_{air} V_{tube} \\ &= 1.21 \text{ kg/m}^3 (0.033 \text{ m}^3) \\ &= 39.9 \text{ gm} \end{aligned}$$

$$\begin{aligned} f_{system} &= (1 / 2\pi) \{1 / [C_{md} (M_{md} + M_{air})]\}^{1/2} \\ &= 20 \text{ Hz} \end{aligned}$$

I also noticed in Figure 2.2 that the resonance peak I would associate with the ¼ wavelength mode of the tube had risen in frequency. The peak in the impedance plot, and in the terminus SPL response plot, occurs at 91 Hz versus the calculated value of 67 Hz. However, in the driver SPL response plot, a sharp null is evident at 70 Hz. This sharp null almost matches the calculated ¼ wavelength frequency of 67 Hz. The drop in the driver resonant frequency and the rise in the first tube resonant frequency is identical in behavior to what is seen in the response plots for a ported box design.

I then started looking at Figures 2.3, 2.4, and 2.5 that show the same measurements as Figure 2.2 but for three different amounts of Dacron Hollofil II stuffing. Converting the amount of stuffing in the test line into a mass per unit volume yields the following densities.

100 gm	=	0.191 lb/ft^3
200 gm	=	0.382 lb/ft^3
300 gm	=	0.573 lb/ft^3

These values span the stuffing density I anticipated using in my final designs. The quarter wavelength resonant frequencies were tabulated for each stuffing density. The terminus SPL phase plots were used to identify the measured resonant frequency for each mode. At the quarter wavelength frequencies, the phase angle passes through +90 degrees or -90 degrees. The impedance curves were used to identify the measured shifted driver resonant frequency. Table 2.3 shows these results.

Table 2.3 : Measured Resonant Frequencies for the Unstuffed and Stuffed Test Line

Mode	Unstuffed Line (Hz)	100 gm of Hollofil Stuffing (Hz)	200 gm of Hollofil Stuffing (Hz)	300 gm of Hollofil Stuffing (Hz)
Driver	22	21	22	22
1/4 Wavelength	94	94	94	91
3/4 Wavelength	214	205	199	193
5/4 Wavelength	343	330	319	306
7/4 Wavelength	475	454	439	428
9/4 Wavelength	598	577	560	545
11/4 Wavelength	727	703	686	669

Looking at the first two rows of Table 2.3, observe that the driver resonant frequency and the ¼ wavelength frequency are essentially constant with increasing stuffing density. The frequency values appear to be independent of the amount of stuffing. This is the frequency range where Bradbury's equations would predict that the air and the fibers are coupled, by a viscous damping coefficient, and the speed of sound is significantly reduced due to the moving fibers. There is no evidence in Table 2.3 that this is occurring. There does not appear to be any dramatic reduction in the speed of sound. At this point, I postulated that at low frequencies the fibers in a transmission line are <u>not</u> moving.

There are two sources of energy dissipation in the stuffed transmission line. First, viscous losses occur as the sound wave moves through the fibrous tangle. The relative motion between the air and the fibers results in viscous forces opposing the air motion. As the sound wave travels along the tube, overcoming these viscous forces transforms mechanical energy into heat.

A second energy dissipation source can be attributed to the traveling sound wave changing from an adiabatic process to a non-adiabatic process. This occurs when heat transfer takes place between the sound wave and the fibrous tangle. The direct result of changing from an adiabatic to a non-adiabatic process is a slight reduction in the speed of sound. The speed of sound in air can be calculated using the following equation.

$$c_{air} = [(n\ p_0) / \rho_{air}]^{1/2}$$

$$n = 1.4 \text{ (adiabatic process)}$$
$$p_0 = 1.013 \times 10^5 \text{ Pa at 20 C}$$
$$\rho_{air} = 1.21 \text{ kg/m}^3 \text{ at 20 C}$$

$$c_{air} = 342 \text{ m/sec}$$

If the process were to become non-adiabatic, the ratio of the specific heats n would decrease slightly. For example, if n decreased from 1.4 to 1.2.

$$n = 1.2 \text{ for a non-adiabatic process}$$
$$c_{fiber} = 317 \text{ m/sec}$$

Starting at the ¾ wavelength mode and moving across the rows in Table 2.3, you can see a slight drop in the frequency of each mode as more stuffing is added to the test line. If the fibers are not moving, then this results from the viscous damping and a non-adiabatic process decreasing the speed of sound. Knowing the length of the tube and the quarter wavelength frequencies, you can calculate the speed of sound for each entry in Table 2.3. Table 2.4 displays the results of this calculation for each stuffing density.

Table 2.4 : Calculated Speed of Sound for the Unstuffed and Stuffed Test Line

Mode	Unstuffed Line (m/sec)	100 gm of Stuffing (m/sec)	200 gm of Stuffing (m/sec)	300 gm of Stuffing (m/sec)
3/4 Wavelength	350	335	325	315
5/4 Wavelength	336	323	313	300
7/4 Wavelength	332	318	308	299
9/4 Wavelength	326	314	305	297
11/4 Wavelength	324	313	306	298

To double-check the assumption that the fibers are not moving, reverse the argument. Assume that the process is adiabatic and that only fiber motion leads to a reduction in the speed of sound. First, calculate the density that would be required to lower the speed of sound from 342 m/sec in air to 297 m/sec, the minimum value in Table 2.4, corresponding to 300 gm of stuffing in the test line.

$$\rho_{air/fiber} = (n\ p_0) / c_{fiber}^2$$

$$n = 1.4 \text{ (adiabatic process)}$$
$$p_0 = 1.013 \times 10^5 \text{ Pa at 20 C}$$
$$c_{fiber} = 297 \text{ m/sec}$$

$$\rho_{air/fiber} = 1.61 \text{ kg/m}^3$$

The difference in the density of air and the combined air and fiber density is 0.40 kg/m^3. Now, multiplying the density difference by the volume in the test line gives the total mass of the moving fibers.

$$M_{fiber} = 0.40 \text{ kg/m}^3 (0.033 \text{ m}^3) = 1.32 \text{ gm}$$

Remember that the air in the test line volume has an approximate mass of 39.9 gm. So for the speed of sound to be reduced to 297 m/sec by fiber motion, only 1.32 gm of the possible 300 gm of fiber is moving. The 1.32 gm of moving fiber must be evenly distributed over the entire volume of the test line. Why would only 1.32 gm, out of a possible 300 gm, be moving? If all of the 300 gm were moving, the speed of sound would drop to approximately 117 m/sec.

Summary :

Based on the preceding argument, I conclude that motion of the fibers in a stuffed transmission line does not occur under normal operating conditions and should not be the basis for a mathematical model. Also, the mathematical model of the air motion in a stuffed transmission line should include two sources of energy dissipation. The model should include viscous damping losses and a slightly reduced speed of sound due to a non-adiabatic process that occurs as the sound waves travel through the fibrous tangle.

Figure 2.1 : Test Transmission Line Layout
All dimensions are in inches.

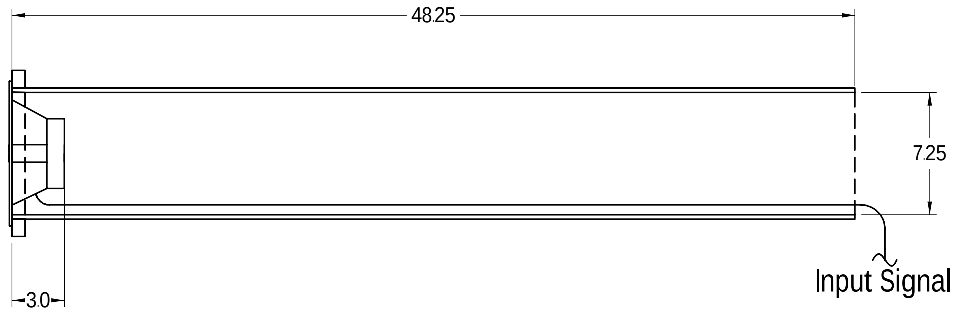

Figure 2.2 : Unstuffed Test Line

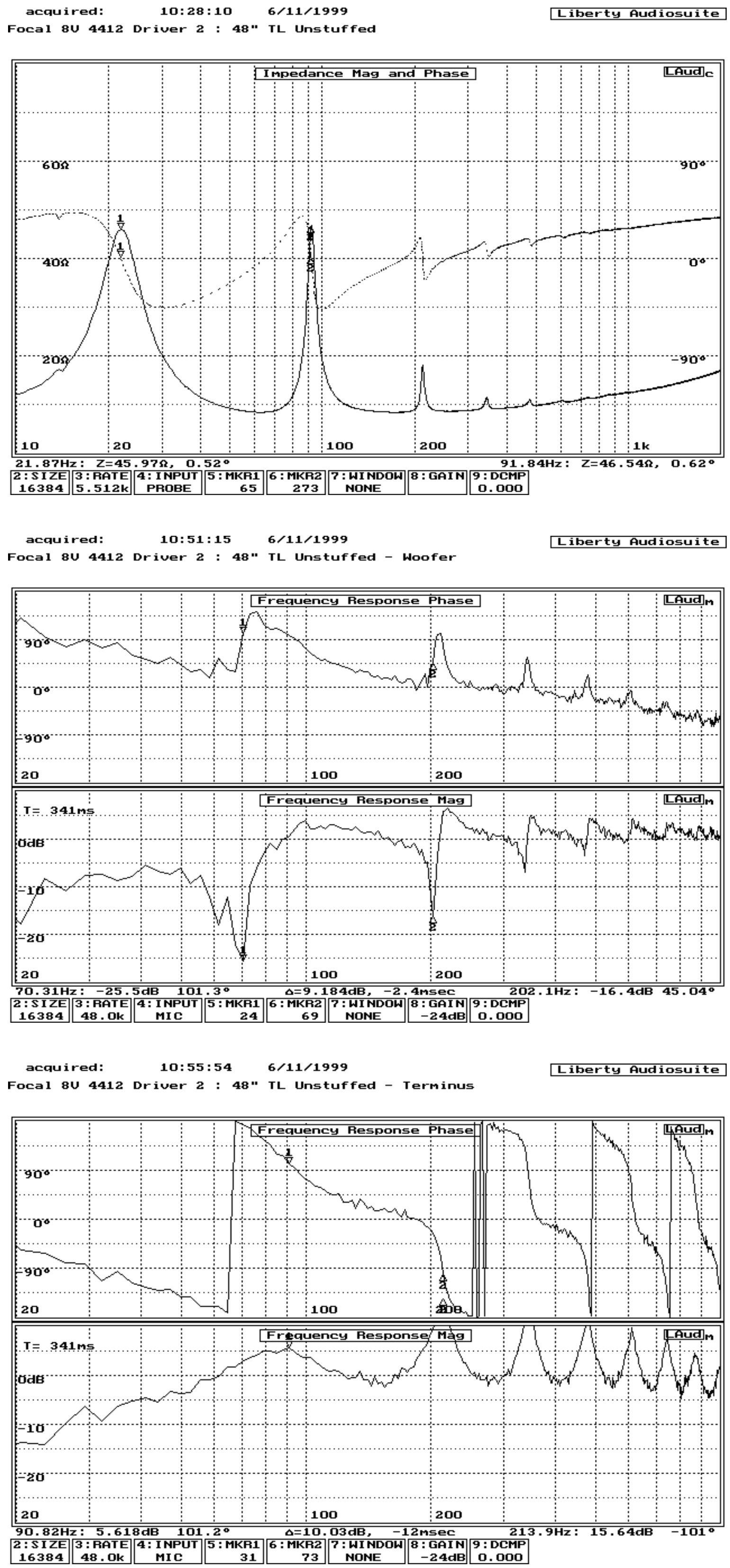

Figure 2.3 : Test Line Stuffed With 100 gm of Dacron Hollofil II

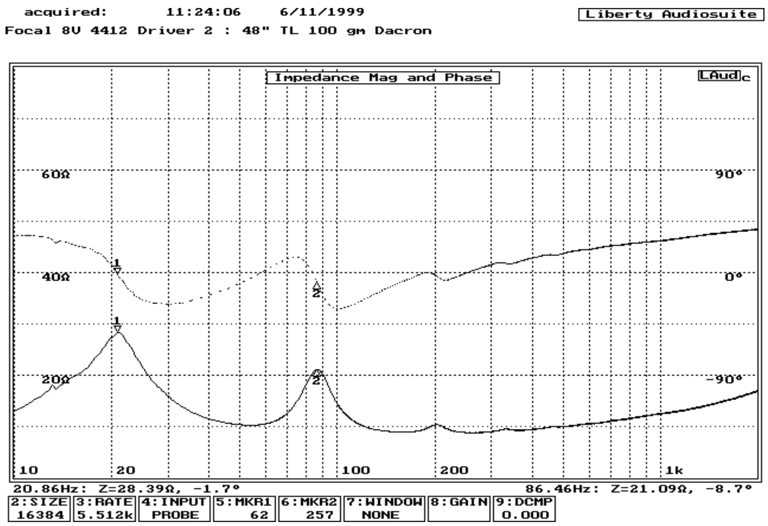

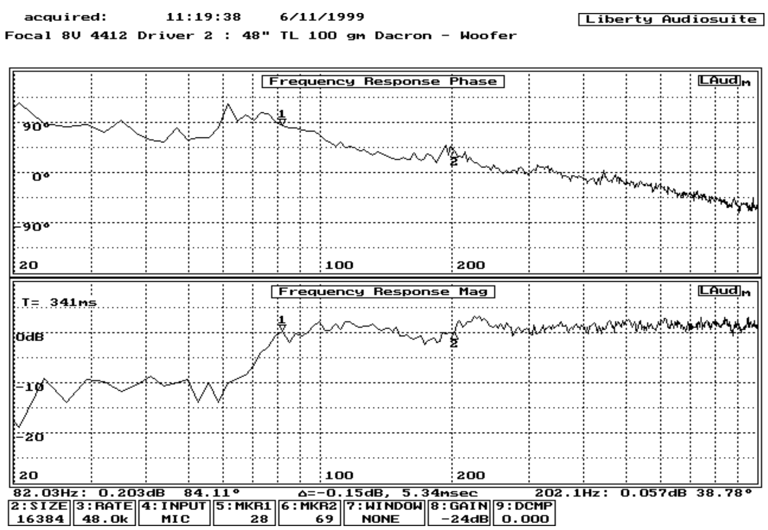

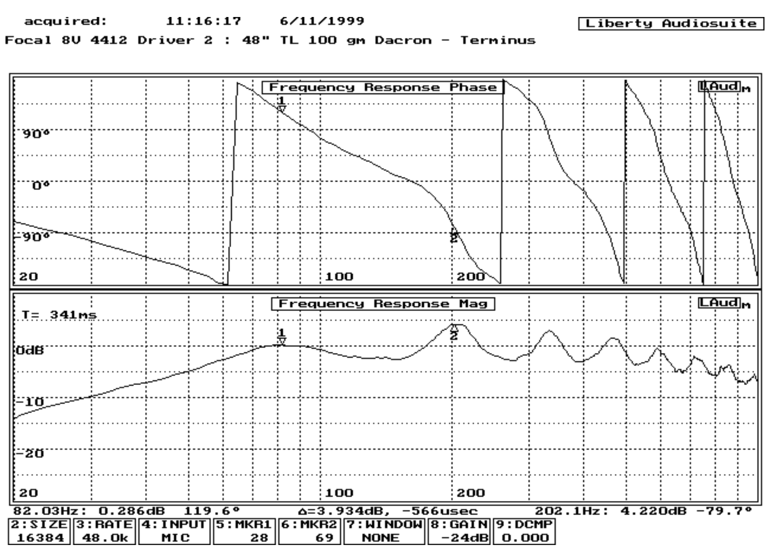

Figure 2.4 : Test Line Stuffed With 200 gm of Dacron Hollofil II

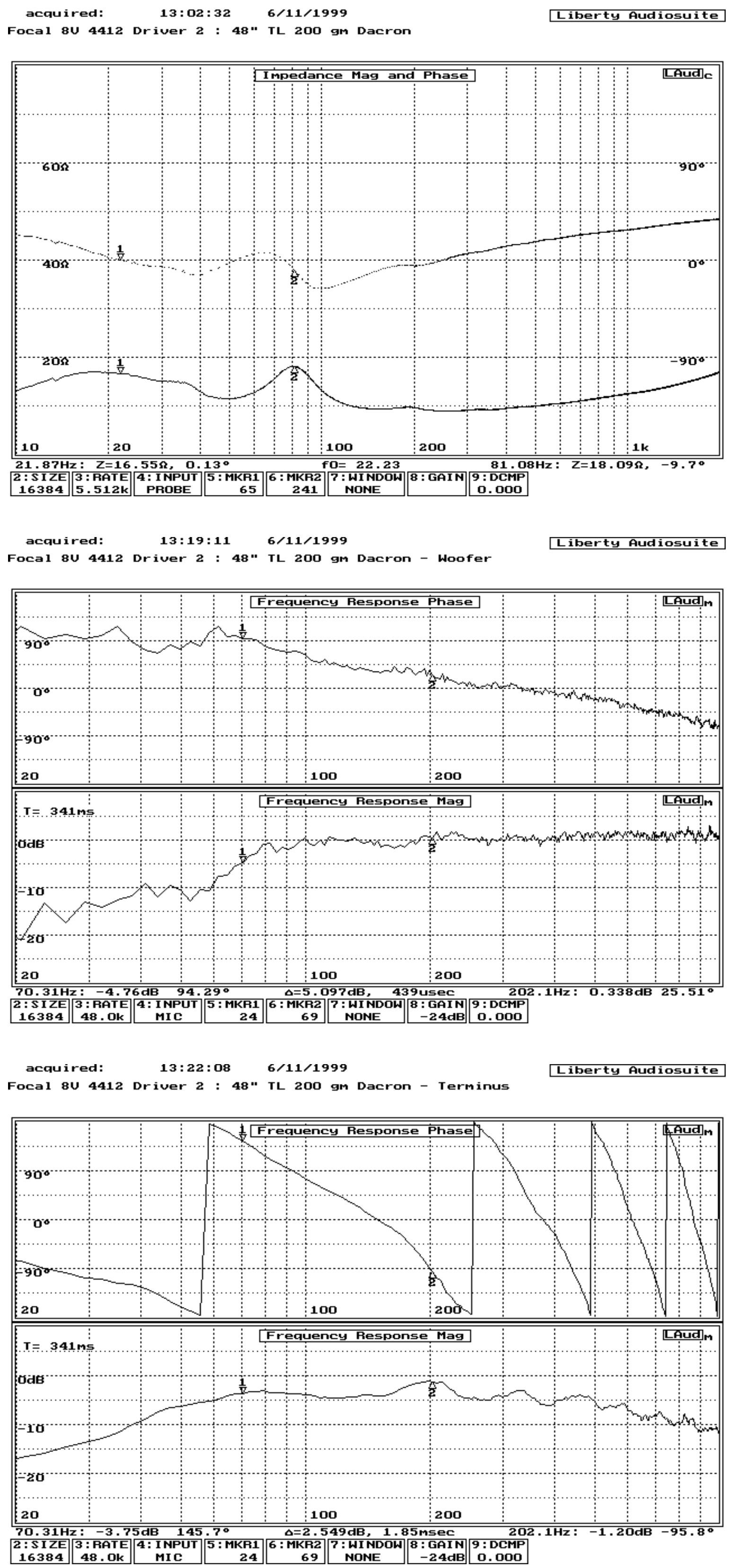

Figure 2.5 : Test Line Stuffed With 300 gm of Dacron Hollofil II